Skeletonisation using an extended Euclidean distance transform

Mark. W. Wright , Roberto Cipolla and Peter. J. Giblin

Abstract

A standard method to perform skeletonisation is to use a distance transform. Unfortunately such an approach has the drawback that only the Symmetric axis transform can be computed and not the more practical smoothed local symmetries or the more general symmetry set. Using singularity theory we introduce an extended distance transform which may be used to capture more of the symmetries of a shape. We describe the relationship of this extended distance transform to the skeletal shape descriptors themselves and other geometric phenomema related to the boundary of the curve. We then show how the extended distance transform can be used to derive skeletal descriptions of an object.

1 Introduction

Skeletonisation is an image processing operation which reduces input shapes to axial "stick like" representations. It has many applications ranging from preprocessing for optical character recognition to use as a shape descriptor in complete object recognition systems. Shape descriptions of this kind are also the subject of renewed interest in the context of robot manipulation and grasping of objects [4]. There are many types of skeletal shape descriptor and many ways in which they can be computed. Of particular note are the family of shape descriptors based on bitangent circles which include the Symmetric Axis Transform (SAT)[5], Smoothed Local Symmetries (SLS)[6], Process Inferring Symmetry Analysis (PISA)[12] and the Symmetry Set (SS)[9]. Differences within this family occur due to what bitangent circles are allowed to contribute to the skeleton and where the skeletal point is drawn in relation to each circle. Of the many methods which can be used to generate these and other skeletal shape descriptors most can be put into four categories: Iterative erosion of the shape boundary *i.e.* thinning, [11], wave propagation from the boundary [5], detection of "local maxima" on a distance transform [1], and analytical methods, for simple shapes, following some form of function approximation, *e.g.* polygon approximation [6].

1.1 The distance transform approach to skeletonisation

The idea behind the distance transform approach is explained in figure 1. If we wish to obtain the symmetric axis transform of the tee shape in figure 1a then we first obtain its distance transform as in figure 1b. This assigns a value to each pixel within the shape equivalent to the distance of that pixel to the nearest point on

BMVC 1994 doi:10.5244/C.8.55

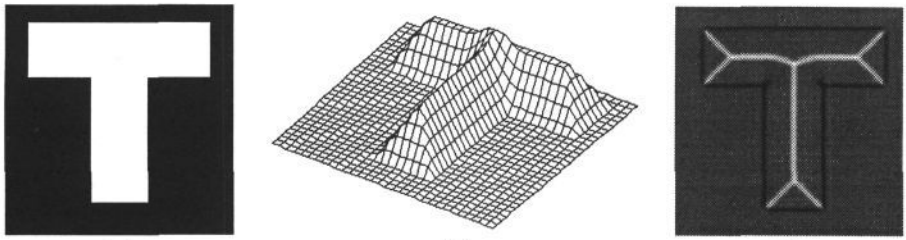

(a) (b) (c)

Figure 1a shows a Tee shape. In figure 1b we see its distance transform, this assigns a value to each pixel within the shape equal to the minimum distance from that pixel to the shape boundary. The Symmetric Axis Transform of a Tee shape, figure 1c, corresponds to the "local maxima" of the distance transform.

Figure 1: The relationship of the SAT to the distance transform

the border. The symmetric axis of the figure corresponds to the "local maxima" of the distance transform as can readily be seen by comparing figures 1b and 1c.

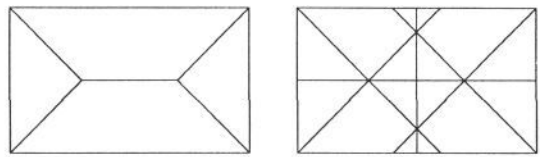

(a) (b)

Figure 2: Limitations of the Symmetric Axis Transform
Figure 2a shows the SAT of a rectangle which is the locus of bi-tangent circles which are contained within the boundary. Figure 2b demonstates that there are many other symmetries which could be expressed.

The main drawback with the distance transform approach to skeletonisation is that it can only produce the Symmetric axis transform (SAT) which does not capture all the potential symmetries of a shape. The SAT is the locus of centres of circles bi-tangent to a shape boundary and *contained completely within that boundary.* In figure 2a we see the SAT for a rectangle, in figure 2b we see the extra symmetries created if all bi-tangent circles are allowed to contribute to the skeleton. In the SAT certain skeletal features are suppressed by the proximity of other boundary segments in a way which can seem counter intuitive. This can be important if the skeleton is to be used in an object recognition system. The presence of an occluding boundary for example can suppress symmetries which would otherwise contribute to the skeleton. This is one reason why the computation of skeletons which capture more symmetries than the SAT is a worthwhile goal.

1.2 Contribution

We address the problem of performing skeletonisation using a distance transform. Our main contribution is to present an *extended* distance transform derived using standard techniques from singularity theory. We demonstrate how this extended distance transform can be used to derive skeletal shape descriptors which capture more symmetries of a shape than can be acquired by the standard distance transform approach. We suggest that studying distance transforms and their role in skeletonisation from the point of view of singularity theory provides an interesting perspective with many valuable new insights.

2 The extended distance transform

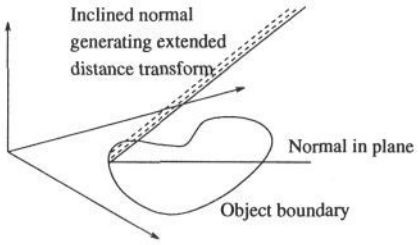

Figure 3: Intuitive explanation of the extended distance transform
We can imagine the extended distance transform being generated by a normal inclined at 45 degrees to the plane as it is swept around the boundary of a shape.

2.1 An intuitive explanation

A central assumption of the distance transform approach is that skeletal axes correspond to the "local maxima" of the Euclidean distance transform. A mathematical analysis of this assumption from the point of view of singularity theory [8] is given below which leads to the introduction of the extended distance transform. However, before embarking on a formal theoretical analysis we feel it is instructive to give an intuitive description of the extended distance transform. Consider a point on a smooth curve as in figure 3. We can imagine tracking this point as it traverses the curve and making note of its inward normal which would sweep across the plane. Now consider this normal raised at an angle of 45 degrees to the plane so that its height above the plane encodes distance along the normal from the boundary. As this new inclined normal is swept along the curve it acts as a generator defining a surface in the space above the plane. It is this surface which is the *extended* distance transform or, as will be defined shortly, the *discriminant*. Figure 4 shows the extended distance transform or discriminant of a circle. It consists of a lower cone which corresponds to the ordinary Euclidean distance transform but extends above this to form another inverted cone. It is this upper portion which has the potential to interact with surfaces from other parts of the

contour and thus define symmetries other than those of the SAT. In figure 5 we see the surface generated by a parabola. There are two significant type of "event" on this surface, *i.e* points where the surface appears "creased" and points where two smooth portions of the surface intersect. The creases correspond to the *evolute* of the curve which is the locus of centres of curvature and the intersections correspond to the skeletal symmetry points.

2.2 Theoretical Analysis

Let $\gamma(t)$ be a regular parameterization of a curve, which we can assume to be unit speed for simplicity of calculation. (That is, $\| (\gamma'(t)) \| = 1$, where the prime denotes differentiation.) The function

$$f(t, x, y) = \| \gamma(t) - (x, y) \|$$

measures the distance from the point $\gamma(t)$ of the curve to the general point (x, y) in the plane. (Compare [8, p.33], where the *square* of f (the 'distance-squared' function) is used. The only purpose of squaring is to make the function differentiable when (x, y) lies on the curve, and for our purposes we can ignore this problem.)

We also consider the family F of functions as follows:

$$\mathbb{R} \times \mathbb{R}^2 \xrightarrow{F} \mathbb{R} \times \mathbb{R}^2$$

$$t, x, y \longmapsto \| \gamma(t) - (x, y) \|, x, y$$

The **critical set** Σ of F is the set of points t, x, y where the Jacobian matrix of F is singular. This is the same as the set of points where f has a critical point, and this occurs precisely when x, y lies on the normal to the curve at $\gamma(t)$. (See [8, p.33].) Thus

$$\Sigma = \left\{ (t, x, y) \mid \frac{\partial f}{\partial t} = 0 \right\}.$$

The **critical locus** or **discriminant** Δ of F is defined by

$$\Delta = F(\Sigma).$$

This is a subset of the target space $\mathbb{R} \times \mathbb{R}^2$.

To see how this relates to the intuitive explanation above, fix t. In Σ there is a line l of points, namely the normal at $\gamma(t)$ but raised to height t. The image $F(l)$ is a line whose projection to the (x, y)-plane is still the normal line. But $F(t, x, y)$, for $(t, x, y) \in l$, is raised above this normal line to a height equal to its distance from the point $(0, \gamma(t))$ at the foot of the normal. Hence the image $F(l)$ is a line through $(0, \gamma(t))$ at 45° to the base plane $t = 0$.

The surface formed by the 45° lines is a *ruled surface* and will usually have singularities. The circle (Fig. 4) is a rather un-typical case here in that all the lines actually pass through a common point. A more typical case is that shown in Fig. 5, where the surface has cusp edges and a swallowtail point.

It is our task first to characterise the singularities of the discriminant surface and then to outline methods for detecting them.

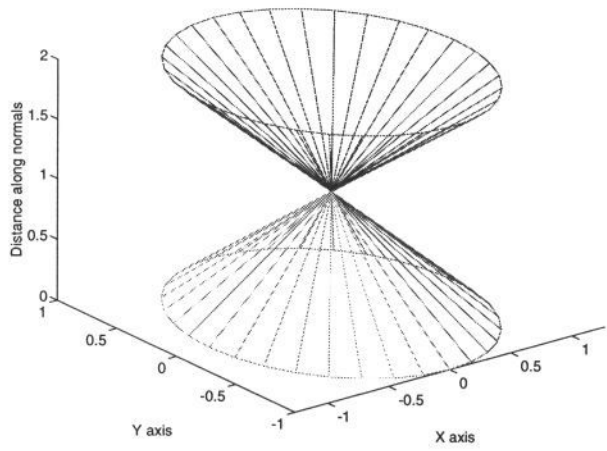

Figure 4: Discriminant for a circle
The discriminant can be thought of as normals to the original curve rising from the plain at 45 degrees. For a circle the discriminant looks like two cones with a solitary singularity at their common apex.

We use Singularity Theory to define the type and position of singularities which occur on Δ. The **critical set** Σ is a smooth surface and so Δ can have only (i) 'multi-local' and (ii) local (or intrinsic) singularities. We proceed to describe these in turn.

2.3 Multi-local singularities

Multi-local singularities are caused by two points of Σ mapping to the same point of Δ. That is, there exist points $(t_1, x_1, y_1), (t_2, x_2, y_2) \in \Sigma$ with $F(t_1, x_1, y_1) = F(t_2, x_2, y_2)$. This clearly requires $x_1 = x_2$ and $y_1 = y_2$, so corresponds to two normals *of the same length*, intersecting at (x_1, y_1). (The lengths are measured from the 'feet' $\gamma(t_1), \gamma(t_2)$ of the normals to the intersection point.)

Equal length normals intersect in the centres of bi-tangent circles, that is, circles tangent to γ at two points, namely $\gamma(t_1)$ and $\gamma(t_2)$. Thus the points (x_1, y_1) generated in this way are part of the Symmetry Set ([9]). The point (x_1, y_1) will also be part of the Symmetric Axis Transform, if the equal normals are the shortest normals from (x, y) to the curve.

2.4 Local singularities

Local (or intrinsic) singularities of Δ are images of points $(t, x, y) \in \Sigma$ where the map $F|\Sigma$ (that is, F restricted to the smooth surface Σ) It turns out that $F|\Sigma$ is singular when $(t, x, y) \in \Sigma$ and (x, y) is at the centre of curvature of γ at $\gamma(t)$. (The calculation for this is almost identical to that in [8, p.33].) This means that (x, y)

is on the evolute which is the locus of centres of curvature (See figure 5). Note that $F(t, x, y)$ only belongs to the Euclidean distance transform when the distance along the normals from (x, y) to $\gamma(t)$ is the shortest among all normals through (x, y). In fact this never happens on the evolute except at cusps (corresponding to maxima and minima of curvature).

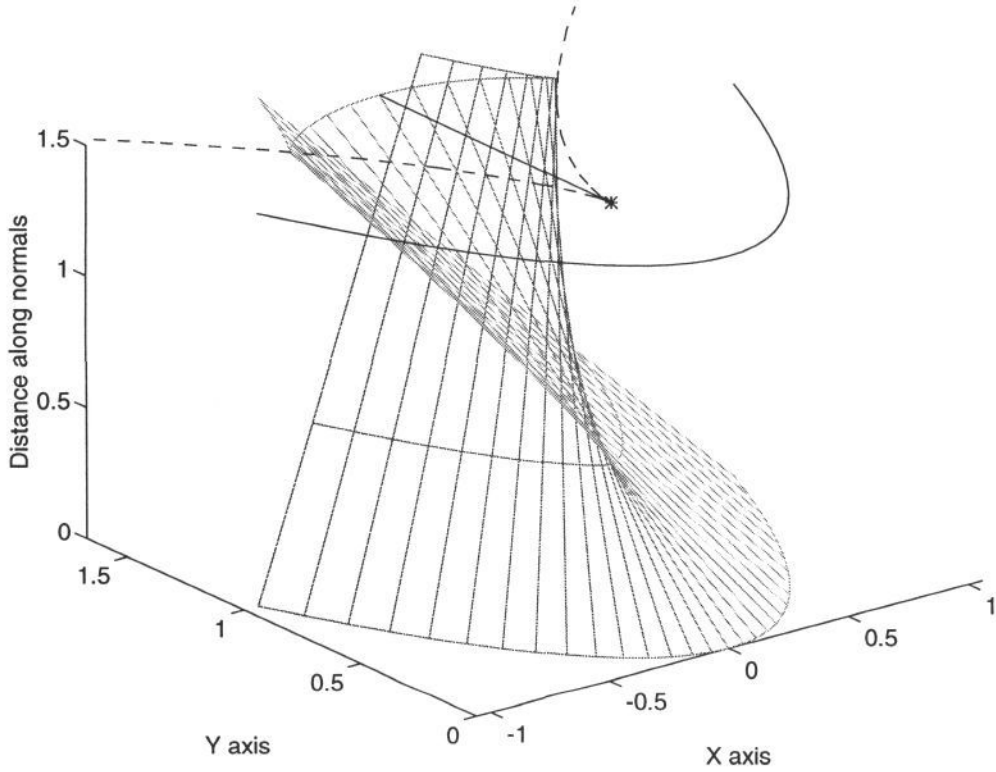

Figure 5: Discriminant for a parabola
The discriminant for a parabola shows a "swallow tail" surface. Above the discriminant is drawn the parabola complete with evolute (dashed line) and symmetric axis (straight solid line). The central symmetric axis corresponds to points of multi-local symmetry on the discriminant, the evolute corresponds to intrinsic singularities which are along the cusped edges of the "swallow tail". The only intrinsic singularity to have a minimum normal distance and therefore to be on the symmetric axis is that corresponding to the cusp on the evolute (asterisk).

2.5 Relevance of analysis

The above analysis is of relevance for three reasons:

1. Singularity theory tells us exactly what type of singularity can exist, under what conditions they occur and their local structure [8, 7, 3, 2].

2. In the literature the artifacts on the Euclidean distance transform which correspond to skeletal points are commonly called "local maxima" [1]. This is a misnomer as strictly speaking they are not local maxima of any variable in the usual sense. Using singularity theory in this context these artifacts can be described simply and formally as singularities of the distance function.

3. The discriminant can be thought of as an *extended* Euclidean distance transform as it contains the EDT but also describes distances along normals which are not minimal. The description of singularities in such cases enables us to detect smoothed local symmetry and symmetry set points. This fact is exploited to advantage in the next section.

3 Computing the discriminant

The process of going from raw image to skeletal description involves three main stages: preprocessing, computation of discriminant and detection of singularities on the discriminant.

3.1 Preprocessing

The input to the algorithm is a grey level image. Edge segments are found using a Canny edge detector and the edge segments from this are chained together using a simple linker. These edge chains are then approximated by cubic B-Splines.

3.2 Computation of Discriminant

We consider the discriminant to be formed from separate smooth sheets. We first dissect the discriminant into these separate sheets and then compute normal distances to all points on these sheets. To dissect the discriminant we compute the evolute of the curve and the curvature extrema. We isolate those parts of the discriminant bounded between two consecutive positive curavature extrema and their corresponding evolutes. These curves are in the form of polygons with floating point vertices. We use a scanline conversion algorithm to find what pixels lie within the boundary of this segment, this registers the sample points to the underlying pixel grid so that heights of the discriminant sheet can be compared with other sheets. For each pixel within the discriminant segment we then find its normal distance to the boundary. At the moment we do this using a root finding algorithm due to Schieder [10].

3.3 Detection of singularities on the discriminant

Once we have computed the discriminant all that remains is to detect its singularities. There are two types of singularity, the intrinsic singularities where the discriminant looks "creased" and multi-local singularities where two smooth sheets apparently "intersect" one another. The intrinsic singularities correspond to the

evolute which has already been detected so the only real problem left is to detect the multi-local singularities. There are many alternatives to find these multi-local singularities but in this initial scheme we choose the simplest which is just to find which sheets of the discriminant overlap *i.e.* which cover the same part of the image plane and then to see which of the pixels within these sheets are at the same height by comparing each corresponding pixel. Those which have the same heights within a small threshold are marked as skeletal pixels.

3.4 Experimental results

Figure 6 depicts a very simple shape to explain how the discriminant is dissected. The numbers denote the control polygon of the round spline boundary. The evolute is the cusped curve inside the shape. One sheet of the discriminant is shaded in between two consecutive positive curvature extrema (asterisks) and the evolute. This comprises of two shaded areas because there is a spline boundary between the extrema. There are a further two partially overlapping segments to be shaded.

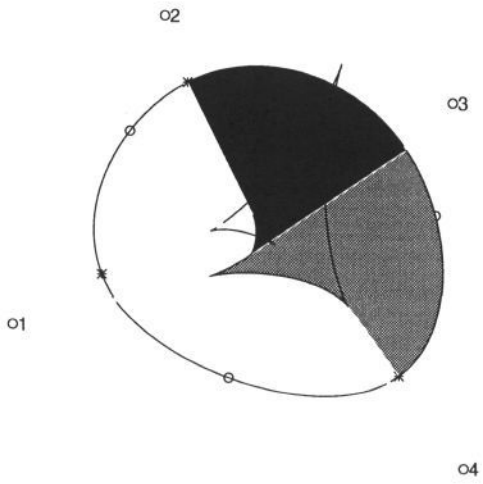

Figure 6: Dissection of Discriminant
Simple spline object (round shape) with control polygon denoted by numbers. Within the shape we see the evolute and one section of discriminant shaded. Section is bounded by positive curvature extrema (asterisks) and evolute.

Figure 7 shows the result of applying the extended distance transform to the skeletonisation of a wrench. In addition to the standard SAT branches running inside the wrench other symmetries are made explicit. Extra branches are formed in the jaws and the end to end symmetry of the jaws is captured by large lateral branches.

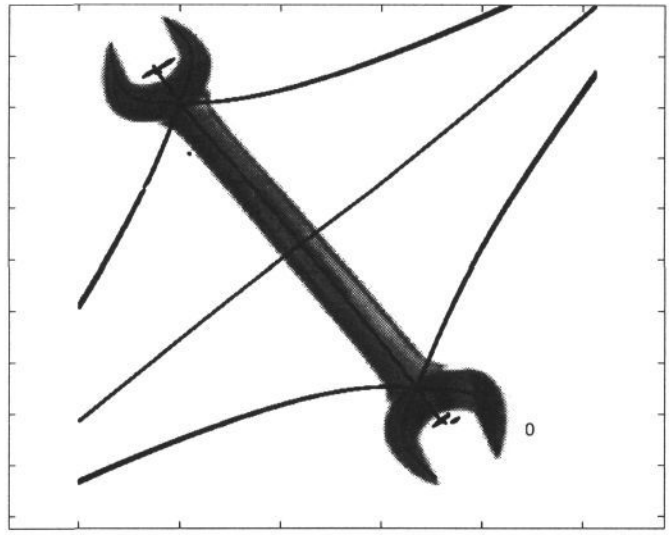

Figure 7: Skeleton of wrench produced by extended distance transform
The skeleton is superimposed on input image. Large lateral branchs are produced denoting the end to end symmetry of the jaws. These would be suppressed in the SAT.

4 Discussion

The method we have used for computing the discriminant is accurate but rather inefficient. Our main concern to date has been to prove the principle of our algorithm, however if this technique is to be viable we need a more efficient method for deriving the discriminant surfaces and detecting their intersection.

One approach would be to compute each smooth surface of the discriminant using separate *constrained distance transforms*. Constrained distance tranforms are used in the literature for tasks such as path planning. These algorithms tend to be more complex than ordinary distance transforms particulary when the distance is propagated from many source pixels. This problem may be circumvented if we take advantage of certain constraints which apply in our case. If an evolute has an inflexion then the corresponding involute (the shape boundary in this case) will have a cusp. By the converse argument if the involute is smooth (which is one of our assumptions) then the evolute will never have an inflexion. So for any section of evolute running between two cusps the curvature of the evolute will have constant sign. This means we can use an ordinary distance transform if we use the following computational sleight of hand. We can initialise the pixels on the evolute with their corresponding radius of curvature. This would mean that the evolute would act as a kind of "wave guide" for the distance transform as it propagated from the source pixels.

5 Conclusion

We have introduced an extended distance transform and demonstrated that it can be used to generate more general skeletal shape descriptors than can be produced using the ordinary distance transform. The current algorithm is promising and although inefficient in terms of speed and memory usage we hope to implement several major improvements shortly. In closing we hope this paper has demonstrated that singularity theory provides a powerful tool in the study of distance transforms and their use in computer vision.

References

[1] C. Arcelli and G. S. di Baja. Finding local maxima in a pseudo-euclidean distance transform. *Computer Graphics Vision and Image Processing*, 43:361–367, 1988.

[2] V.I. Arnol'd. Wave front evolution and the equivalent morse lemma. *Communications on pure and applied mathematics*, 29:557–582, 1976.

[3] T.F. Banchoff and P.J. Giblin. Global theorems for symmetry sets of smooth curves and polygons in the plane. *Proceedings of the Royal Society of Edinburgh*, 106A:221–231, 1987.

[4] A. Blake, M. Taylor, and A. Cox. Grasping visual symmetry. In *Fourth International conference on computer vision*, pages 724–733, 1993.

[5] H. Blum. Biological shape and visual science (part 1). *Journal of Theoretical Biology*, 38(2):205–287, February 1973.

[6] M. Brady and H. Asada. Smoothed local symmetries and their implimentation. A.I.Memo 757, MIT, February 1984.

[7] J.W. Bruce and P.J. Giblin. Growth, motion and 1-parameter families of symmetry sets. *Proceedings of the Royal society of Edinburgh*, 104A:179–204, 1986.

[8] J.W Bruce and P.J. Giblin. *Curves and singularities.* Cambridge University Press, second edition, 1992.

[9] P.J. Giblin and the late S.A. Brassett. Local symmetry of plane curves. *American mathematical monthly*, 92(10):689–707, 1985.

[10] Andrew. S. Glassner. *Graphics Gems.* Academic Press, 1990. ISBN 0-12-286165-5.

[11] C. J. Hildich. Linear skeletons from square cupboards. In B.Meltzer and D.Michie, editors, *Machine Intelligence IV*, chapter 22, pages 403–420. Elsevier,New York, 1969.

[12] M. Leyton. A process-grammar for shape. *Artificial Intelligence*, 34:213–247, 1988.